Chapter 3

Kinetics of Growth of Iron Boride Layers on a Low-Carbon Steel Surface

Enrique Hernández-Sánchez and
Julio Cesar Velázquez

Additional information is available at the end of the chapter

http://dx.doi.org/10.5772/intechopen.73592

Abstract

This chapter describes the boriding process and the parameters that govern it. It also describes the features of the obtained layers and the main applications of materials treated with this hardening process. The kinetics of growth of the Fe_2B face is described using a mathematical model, in which the evolution of the growth of the boride layers is assumed to be controlled by the boron diffusion by means of a dimensional analysis of Fick's second law. The evolution of the growth of the Fe_2B face on a low-carbon steel surface is illustrated by contour diagrams that involve the main variables of the process (time and exposure temperature). This type of diagrams allows the optimization of the process as a function of the treatment parameters.

Keywords: boriding, iron boride, kinetics, surface layers, low carbon steel

1. Introduction

Boriding is a thermochemical treatment by which it is possible to obtain extremely hard layers. Through boriding, it is possible to enhance the wear resistance and corrosion resistance of acid and/or alkaline media.

Through boron diffusion in the surface of a metal or alloy, a dense zone of borides of the base metal with high mechanical properties is expected to appear.

The relatively small size of the boron atom (8.7×10^{-2} nm) allows it to diffuse in a high variety of metals, such as iron alloys, nickel, nickel alloys, cobalt alloys, titanium and titanium alloys [1].

Boron reacts with metals to form intermetallic compounds that enhance surface hardness and increase wear resistance [2].

The formation of iron borides during the boriding of steel alloys, consists of two main reactions. First, nucleation of the iron boride particles on the surface of the substrate takes place; then, a diffusive process occurs where the layer starts to grow on the metallic surface.

The thickness of the achieved layers is highly dependent on the temperature at which the process is realized and on the exposure time. During the diffusion process and the subsequent absorption of boron atoms, the formation of interstitial solid solutions, which can be single-or double-face Fe_2B or Fe_2B/FeB, occurs.

The formation of the FeB and Fe_2B faces can be explained by the low solid solubility of atomic boron in steel. When this value is not exceeded, the boron can only be present in the iron matrix as a solid solution. However, when the limit of solubility is reached, the Fe_2B face is formed and grows with a flat front during the boriding process if enough active boron is provided [2].

During the diffusion process, borides are formed in grain boundaries. Also, as the transportation of boron atoms through the grain boundaries increases, the formation of a flat front can be disturbed and the Fe_2B face will have an irregular morphology similar to a saw-toothed shape.

Nevertheless, although the Fe_2B face is formed with a saw-toothed morphology, one should note that, once a continuous face of Fe_2B is formed, it will act as a diffusion barrier, this is because of some properties of this boride, such as a high melting point and high stability at high temperatures, which are characteristics of the compounds known as inhibiters of diffusion. Therefore, it is expected that the Fe_2B face could be a barrier for boron or iron diffusion.

On the other hand, to obtain the uninterrupted growth of the Fe_2B face, a continuous flux of boron or iron is necessary, depending on the side of the Fe_2B/Fe interface on which the diffusion occurs. Likewise, by assuming that the growth of the Fe_2B boride occurs from the surface to the interior of the substrate (that is, in the Fe/Fe_2B interface) and that the boron flux has to pass through the previously formed diffusion barrier of Fe_2B, the Fe-B relation will not have the required proportion to continue forming the Fe_2B-type boride. The proportion of boron will be lower because the active boron is accumulated at the back at the Fe_2B face. This sequence of events could explain why FeB is generally the outermost face in steels exposed to boriding for long periods of time and high temperatures where the diffusion speed is higher.

In that sense, a metallic matrix with a high concentration of alloy elements could enhance the formation of a double-face FeB/Fe_2B as a consequence of the growth of a continuous Fe_2B face, which will act as a diffusion barrier.

1.1. Mechanical, physical, and chemical properties of iron borides

The structure of borides is determined by the size of the boron atom and the size of the atoms of the material in which it is diffused, as well as its strong tendency to mix with them. Boron is highly soluble in materials with a small atomic volume, such as iron and its alloys. Depending

http://dx.doi.org/10.5772/intechopen.73592

on the characteristics of the substrate and boron's potential to be employed during the treatment, it is possible to generate single-face (Fe_2B) or double-face (FeB/Fe_2B) layers on the surface, which will be hard layers with a saw-toothed morphology.

According to Matuschka [3], the chemical composition of iron borides can be obtained from the Fe/B faces, as shown in **Figure 1.**

The FeB face has 16.2% boron by weight and has an orthorhombic crystalline structure, with lattice parameters a = 0.4053 nm, b = 0.5495 nm, and c = 0.2946 nm. On the other hand, the Fe_2B face contains approximately 8.83% boron by weight with a tetragonal crystalline structure and lattice parameters a = 0.5978 nm, and c = 0.4249 nm.

Both intermetallic compounds have a preferential crystallographic direction of growth [001] because the atomic density is higher in that direction.

The nature of the layer formed depends on the boron potential that surrounds the sample.

It has been established that for low-to-medium boron potentials, preferential growth of the Fe_2B face [4] is expected. The formation of the FeB face requires a high boron potential, in addition to the influence of the alloying elements content in the steel, especially chromium, nickel, vanadium, tungsten and molybdenum [5].

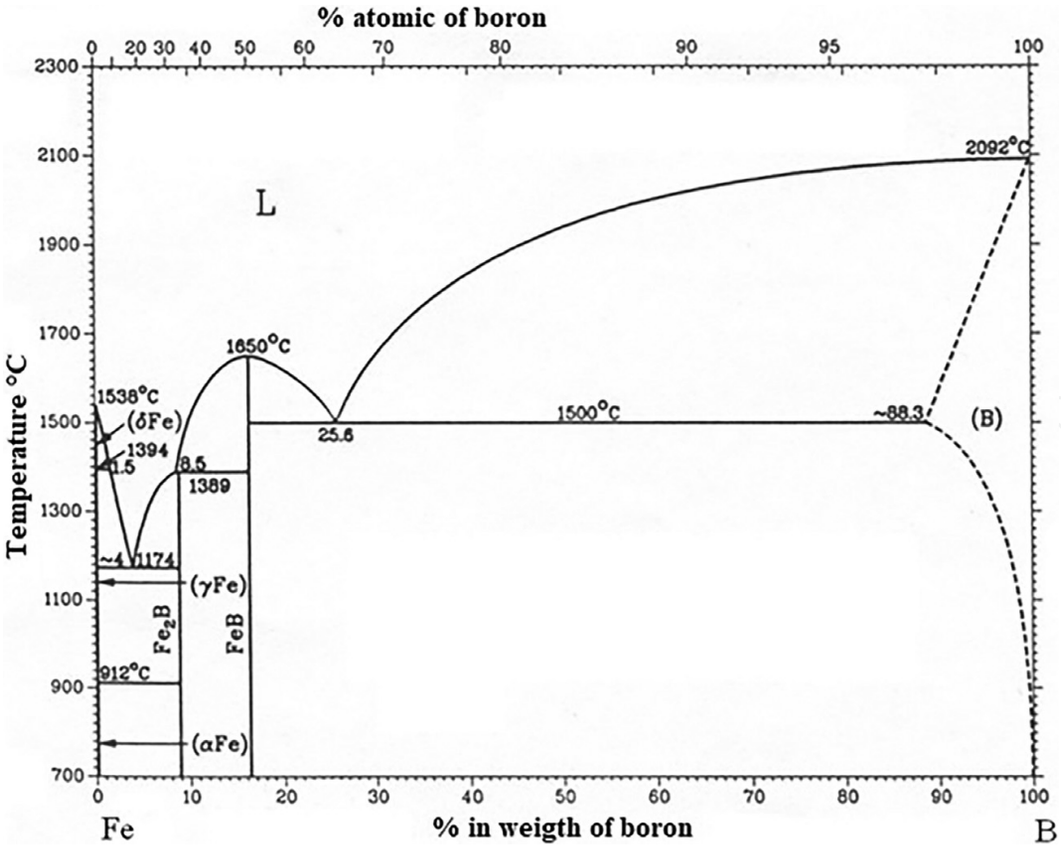

Figure 1. Iron-boron faces diagram [3].

The presence of oxygen during the treatment favors the formation of porosity in the borides because oxygen reacts with the carbon of the boriding agent (B_4C) and forms CO and a boron oxide, which obstructs the boriding process; thus, the formation of boron oxides consumes the active boron as B_2O_3 [6].

The porosity of the boride layers represents points of stress concentration, which indicates degradation of the mechanical properties of the layers **Table 1** shows some chemical and mechanical properties of the iron borides.

Properties	FeB	Fe_2B
Density (g/cm^3)	6.75	7.43
Thermal expansion coefficient (ppm/K)	23 in the range of 200–873 K	7.65–9.2 in the range of 373–1073 K
Hardness (HV)	1900–2200	1800–2000
Young's modulus (GPa)	590	285–295
Fatigue resistance		It can increase in 33% in layers up to 40 μm in thickness (185 a 245 N/mm^2)

Table 1. Some chemical and mechanical properties of the iron borides.

1.2. Influence of the alloying elements on the growth of borides

The morphology of the growth front of the iron borides is determined mainly by the alloying elements in the substrate and not by the preferential crystalline growth of the layers in the [001] direction, as was initially proposed [3, 7]. A saw-toothed front is observed mainly in pure iron and low-to-medium carbon steels. However, in high-carbon-content steels, the thickness of the layers tends to decrease because carbon atoms do not diffuse on the boriding faces and tend to be pushed into the matrix of the substrate, thereby forming a diffusion zone just below the layer.

Elements like nickel and chromium in concentrations of up to 9% and 6% by weight, respectively, favor the formation of iron borides with flat growth fronts.

Segregation of the alloying elements occurs from the substrate to the boride layers by forming intermetallic compounds with active boron. The atoms of the alloying elements diffuse in the layer substitutionally and tend to concentrate in the tips of boride columns, causing a reduction in the active boron flow in this zone; this is why iron-boron reactions lose importance and the size of the columns decreases progressively.

Figure 2 shows three microphotographs of iron boride layers obtained from three ferrous substrates, where different morphologies of the growth fronts as a function of the alloying elements of each material can be observed.

1.3. Applications of the boriding process

The use of boriding as a surface-hardening process greatly improves the mechanical, physical and chemical properties of the surface of materials exposed to it.

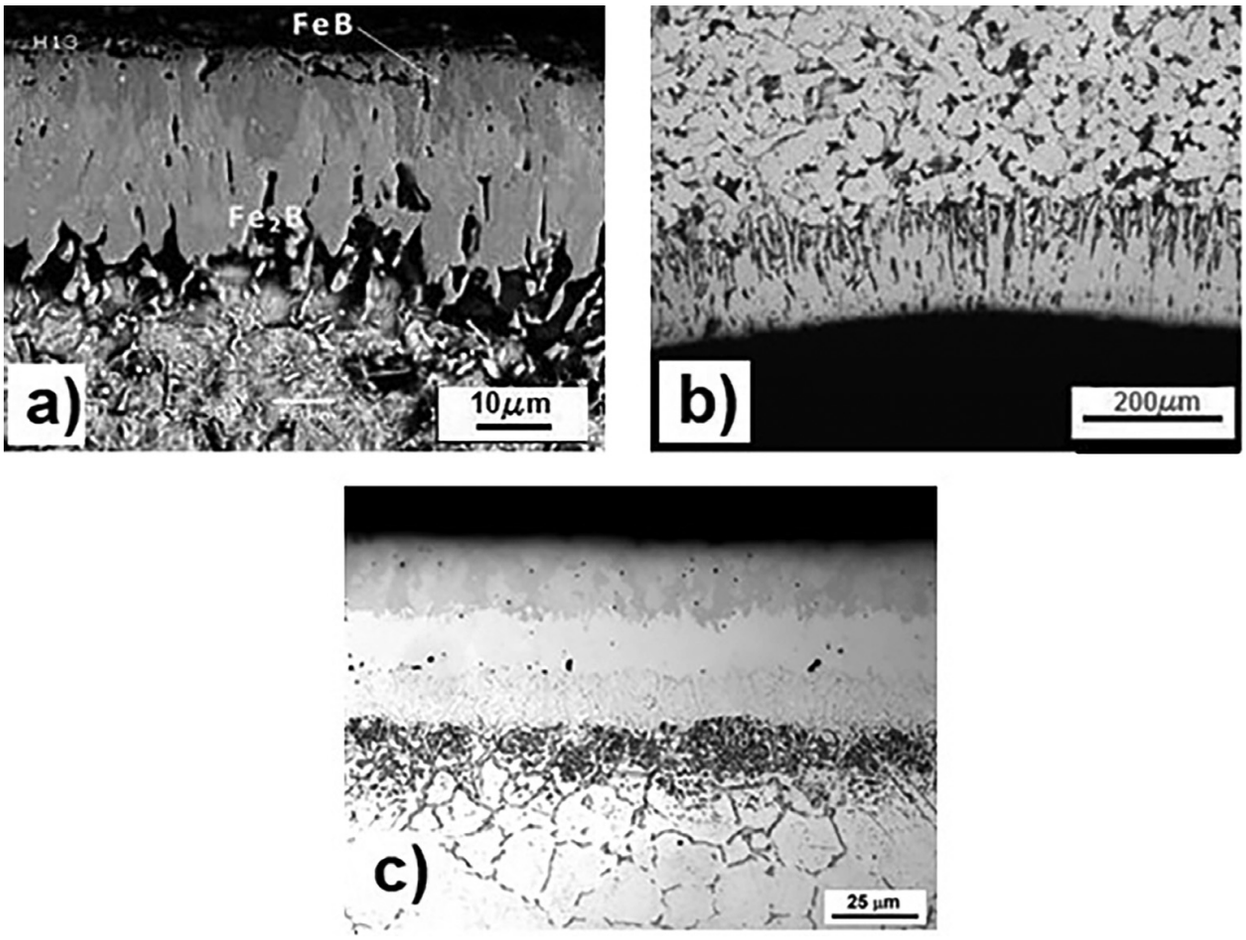

Figure 2. Morphology of the boride layers of different ferrous alloys: a) AISI H13, b) AISI 1018 and c) AISI 316.

Table 2 shows some materials exposed to boriding and their properties before and after the process.

Steel	Surface layer	Hardness (HV) Before and after treatment		Ref
(AISI)		Before	After	
5140	Fe_2B	253	1198–1739	[1]
4340	FeB-Fe_2B	300	1077–1632	[1]
D2	FeB-Fe_2B	660	1500–2140	[1]
1018	Fe_2B	126	1800–1843	[2]
9840	FeB-Fe_2B	265	1600	[9]
1018	Fe_2B	120	1700	[9]
4140	FeB-Fe_2B	290	1446–1739	[12]

Table 2. Materials exposed to boriding and the resulting properties.

In industrial applications, a single Fe_2B face is more desirable than a double FeB/Fe_2B-type face layer because of the formation of cracks in the interface of growth, which are caused by the

difference in the thermal expansion coefficients of the two faces. Additionally, the substrate generates residual stresses of compression and tension during the growth of borides.

1.4. Kinetics of growth of iron borides

1.4.1. Influence of experimental conditions on the formation of the iron boride layers

In order to control the boriding process and achieve its automatization, it is essential to know the kinetic parameters that govern it [8]. Some mathematical models have been developed to establish the variables that affect the kinetics of the boride layer formation process and thus generate a layer thickness according to the needs of the operation [9].

The thickness of the resulting layer has to be determined as a function of the base material. According to the industrial application, a layer thickness in the range of 15 to 20 μm (thin layers) is employed as protection against adhesive wear (stamping die, extrusion tools, etc.). For erosion-corrosion protection, it is recommended to work with relatively high-thickness layers (50 to 250 μm) formed on low-alloy steels. In the case of high-alloy steels, the optimum layer thickness is between 25 and 76 μm [10].

In this chapter, the evolution of boron diffusion on Fe_2B is described by considering the experimental data of layer growth, obtained during the application of the powder-pack boriding process to a low-carbon steel. Additionally, the kinetic growth of the Fe_2B layer can be analyzed by the estimation of its thickness as a function of the processing time in the examined temperature range.

1.4.2. Diffusion model

During the boriding process, the layer thickness increases as the treatment temperature and time increase, maintaining a parabolic relation between the thickness of the layer and the time of treatment [11].

From experimental layer thickness data, it is possible to determine the parabolic growth constants. It is necessary to assume that the rate of growth is controlled by boron diffusion by means of a dimensional analysis of the second law of Fick

$$\frac{\partial C}{\partial t} = D\frac{\partial^2 C}{\partial X^2} \tag{1}$$

In general, the deduction of Fick's second law is very complex; nevertheless, a solution can be considered as:

$$C_{(x,t)} = A + Berf\left(\frac{x}{2\sqrt{Dt}}\right) \tag{2}$$

The expression of Eq. (2) considers a case where the boron concentration profile in the Fe_2B face is a lineal function, as shown in **Figure 3**.

http://dx.doi.org/10.5772/intechopen.73592

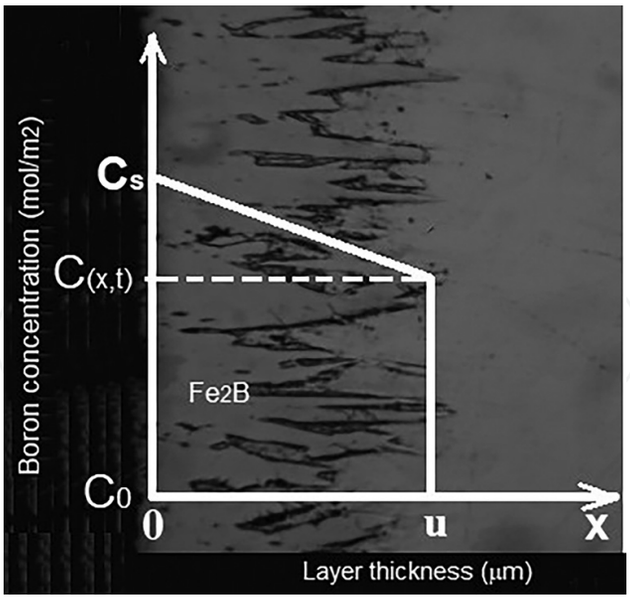

Figure 3. Schematic representation of the boron concentration profile on the Fe_2B layer.

The initial and boundary conditions for the interval $0 \leq x \leq u$ can be established from the concentration profile, as shown in **Figure 3**.

The initial conditions are:

$$x = 0, C_{(x,t)} = C_s \tag{3}$$

Thus, the substitution of x y $C_{(x,t)}$ in Eq. (2) results in:

$$C_s = A + B(0), \quad A = C_s \tag{4}$$

The boundary conditions are established as:

$$x = u; C_{(x,t)} = C_0 \tag{5}$$

Then, by substituting Eq. (5) in Eq. (2), it can be established that:

$$C_0 = C_s + Berf\left(\frac{u}{2\sqrt{Dt}}\right) \tag{6}$$

Then, extracting B from Eq. (6) results in:

$$B = \left(\frac{C_0 - C_s}{erf\left(\frac{u}{2\sqrt{Dt}}\right)}\right) \tag{7}$$

Replacing A and B in Eq. (4) results in:

$$C_{(x,t)} = C_s + \left(\frac{C_0 - C_s}{erf\left(\frac{u}{2\sqrt{Dt}}\right)}\right) \operatorname{erf}\frac{x}{2\sqrt{Dt}} \tag{8}$$

On the other hand, it is well known that:

$$\lim_{u\to 0} erf\left(\frac{u}{2\sqrt{Dt}}\right) \Rightarrow 0 \tag{9}$$

$$\lim_{u\to \infty} erf\left(\frac{u}{2\sqrt{Dt}}\right) \Rightarrow 1 \tag{10}$$

Finally, the boron concentration in the Fe_2B layer is expressed as follows:

$$C_{(x,t)} = C_s + (C_0 - C_s) erf\left(\frac{x}{2\sqrt{Dt}}\right) \tag{11}$$

When the layer thickness (x) is extracted from Eq. (11), it can be rewritten as:

$$x^2 = \left[2\sqrt{D}\, erf^{-1}\left(\frac{C_{(x,t)} - C_s}{C_0 - C_s}\right)\right]^2 t \tag{12}$$

where:

$C_{(x,t)}$ is the boron concentration at a distance x at a time t (mol/m^3).

C_s is the boron concentration at the surface of the sample (mol/m^3).

C_0 is the boron concentration at the substrate (mol/m^3).

x is the thickness of the layer [μm].

t is the treatment time [s].

D is the boron diffusion coefficient in the Fe_2B layer [m^2/s].

erf is the Gauss error function [11].

Consequently, for a distance x at any time t, the relation between the boron concentrations and the diffusion coefficient remains constant, as shown in Eq. (13). Therefore, Eq. (12) takes the form of Eq. (14).

$$K = \left[2\sqrt{D}\, erf^{-1}\left(\frac{C_{(x,t)} - C_s}{C_0 - C_s}\right)\right]^2 \tag{13}$$

K is the constant of parabolic growth [m^2 s^{-1}], expressed by Eq. (13).

$$x^2 = Kt \tag{14}$$

x is the layer thickness [m] and K depends on the boron diffusion coefficient in the Fe_2B layer and the boron concentration gradients through the thickness of the Fe_2B layer, and t is the treatment time [s].

Considering that for the treatment conditions (time and temperature), the square of the layer thickness changes linearly with time, the relation between the constant of parabolic growth (K), the activation energy, and the temperature of the process can be expressed as an Arrhenius model:

$$K = K_o \exp\left(-\frac{Q}{RT}\right) \tag{15}$$

where K_o is a pre-exponential factor that depends on the boron potential of the boron source surrounding the substrate during the thermochemical treatment [$m^2\ s^{-1}$] and R is the universal constant of ideal gases [8.3144 J $mol^{-1}\ K^{-1}$].

The activation energy needed to make the diffusion process occur in the Fe_2B layer can be estimated by plotting Eq. (15) in logarithmic form, as follows:

$$\ln K = \ln K_o - \left(\frac{Q}{RT}\right) \tag{16}$$

Figure 4 shows the graph $\ln K$ *vs* $1/T$, where the resulting straight line can be observed.

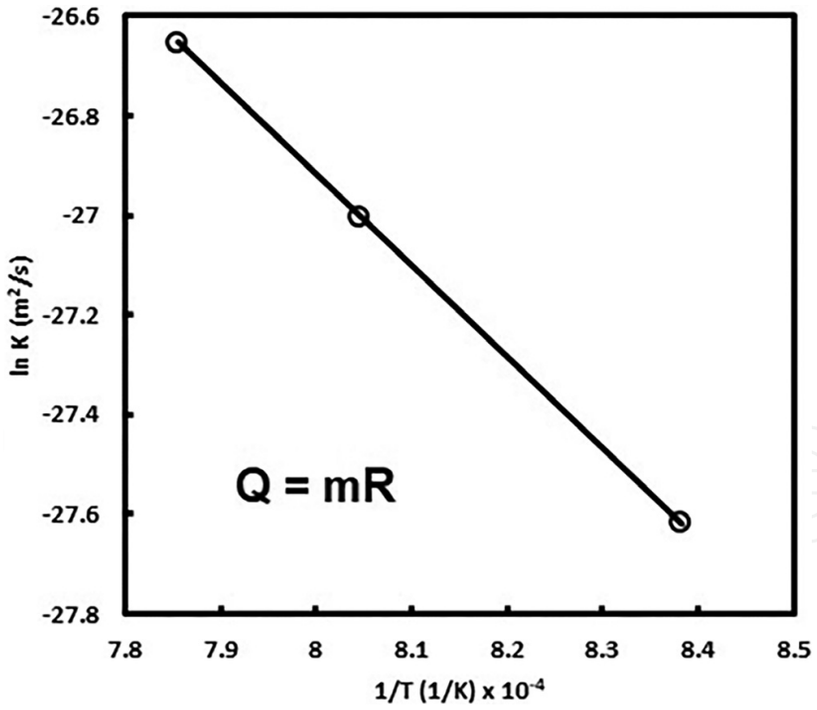

Figure 4. Graph $\ln K$ *vs* $1/T$.

Finally, after the constant of parabolic growth (K) and the pre-exponential factor (K_0) have been determined for the specific range of experimental conditions (temperature and time), Eq. (14) can be transformed to:

$$x = \sqrt{K_0 - \exp\left(\frac{-Q}{RT}\right)\mathrm{t}} \tag{17}$$

Eq. (17) describes the relation between the layer thickness and the experimental parameters of time and temperature. According to Eq. (17), the behavior of the layer thickness as a function of the treatment conditions can be described by means of contour diagrams [12], based on the previously established empirical relations, between the process parameters and the thickness of the boride layers. These contour diagrams are especially useful when the aim is to optimize the boriding process, since the experimental parameters can be estimated as a function of the desired layer thickness.

Figure 5 shows a contour diagram that shows the experimental conditions of time and temperature as a function of the layer thickness.

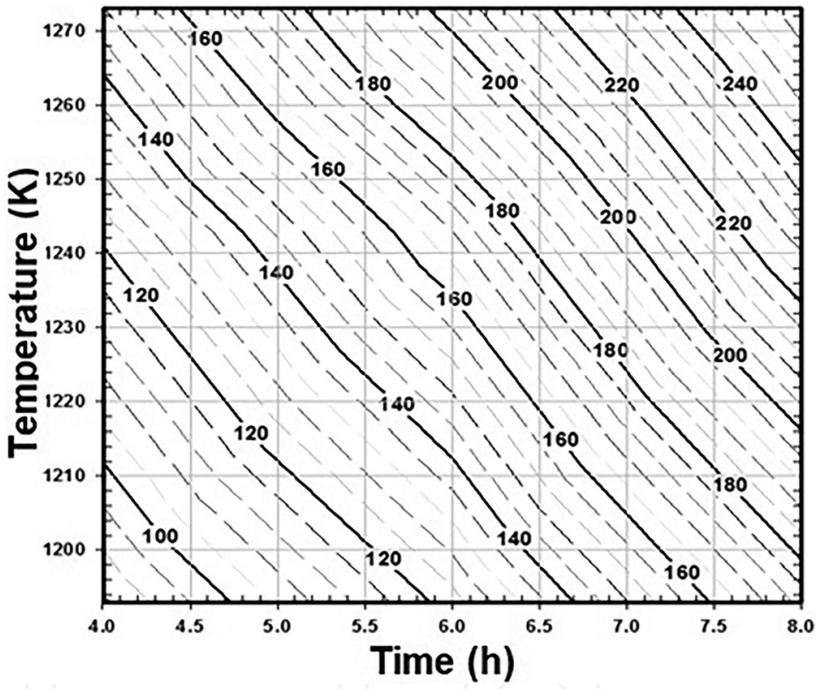

Figure 5. Contour diagram that describes the behavior of the iron boride layers as a function of the experimental conditions.

The contour diagram can be an excellent tool for determining the best treatment conditions for the generation of the determined layer thickness after the analysis of the experimental results.

1.4.3. Experimental considerations

Before to the experimental process it is necessary to observe certain considerations in order to obtain the best results. The next issues are the steps to follow during the powder-pack boriding process:

1.4.3.1. Establishment of treatment conditions

Boriding process takes place in a range of temperatures from 800 to 1100°C and exposure times between 1 and 12 h, depending on the chemical composition of the substrate. The treatment

conditions are the main features that determine the characteristics of the layers such as thickness, hardness and Young's modulus.

1.4.3.2. Selection and preparation of the material

Boriding process can be applied to a several metallic materials, nevertheless, it is very important to consider that resulting layers will be affected by the chemical composition of the substrate. Also the dimensions of the samples have to be considered according to the internal dimensions of the furnace.

Samples should be metallographically prepared in order to allow the correct diffusion of the boron. The metallographic process consists on grind the samples by means of SiC emery paper from 60 to 600 mesh to obtain a good final roughness after the boriding process. Samples should be clean preferably by sonication to remove any impurity.

1.4.3.3. Packaging of the samples

Samples should be packaged in a SS container as shown in **Figure 6**, it is very important to make sure that the samples are perfectly covered with the powder mixture to avoid the oxidation. The powder mixture can be of different composition but the most commonly used is CSi 90% wt., B_4C 5% wt., and KBF_4 5% wt.

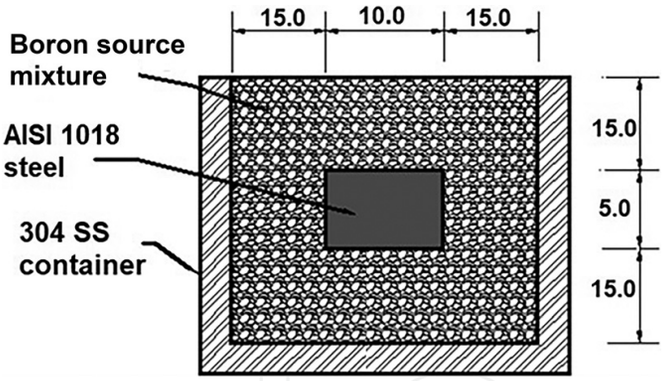

Figure 6. Schematic representation of the location of the samples inside the boriding mixture (dimensions in millimeters).

1.4.3.4. Furnace requirements

For the application of the powder-pack boriding it is no necessary a special furnace, so that, it is enough a conventional furnace with temperature control. The temperature of the furnace has to be set according to the pre-established value and let that the furnace is to stabilize.

1.4.3.5. Thermochemical treatment

Once the temperature in the furnace is stable, the SS container with the samples is set into it and after the temperature stabilizes again, the process starts.

After the process time, the SS container with the samples is removed from the furnace and cooled to room temperature in quiet air. Then, samples are cleaned with scotch fiber to remove impurities.

1.5. Application example

1.5.1. Treatment conditions

In this application example, three temperatures (1173, 1223, and 1273 K) and three exposure times (1.5, 3, and 5 h) for each temperature were considered, as treatment conditions.

Experimental conditions are the main features that determine the layer's properties such as thickness, hardness and Young's modulus.

1.5.2. Sample material

Cylindrical samples of AISI 1018 (structural Steel) with 10 mm diameter and 5 mm length were considered as the samples for the experiments. Their chemical composition was as follows: 0.15–0.20%wt. C, 0.6–0.90%wt. Mn, 0.04%wt. P max., 0.15–0.30%wt. Si and 0.05%wt. S max. The hardness of annealed AISI 1018 is 126 HB; nevertheless, after boriding a surface layer, high hardness can be expected (2000 HV).

1.5.3. Thermochemical treatment of powder-pack boriding

Powder-pack boriding was considered as a good alternative to generate hard layers, because it is a low-cost process and the resulting layers are of reasonable quality. The process consists of packing the samples in a powder mixture rich in boron inside of a stainless steel box.

The powder-pack method offers some advantages over others techniques because it does not require the presence of an inert atmosphere, so that it can be carried out in a conventional furnace. The powder mixture generally consists of 5%wt. B_4C which acts as a boron donor, 5% wt. KBF_4 which acts as an activator and 90%wt. SiC which acts as a diluent [13].

The samples′ location inside of the SS box is of great importance because the amount of boron that diffuses to the samples depends on the amount of boron in the source surrounding the samples [13]. In addition, an insufficient amount of boriding agent can facilitate the presence of oxygen, which would allow the formation of iron oxides on the surface of the material. A boriding agent thickness of 10 mm around the samples is considered enough to protect them from oxidation during the process because of the absence of an inert atmosphere.

The chemical reaction that takes place during the boriding process is as follows:

$$B_4C + 3SiC + 3O_2 \xrightarrow[SiF_4]{BF_3} 2Si + SiO_2 + 4CO \tag{18}$$

It is clear that KFB_4 aggregated as an activator does not interfere in the chemical reaction, so that it does not contribute free boron during the thermochemical process.

1.5.4. Physical characterization of the hardened steels

Figure 7 shows the process diagram of the physical characterization of the Fe_2B layers obtained on the surface of the ASISI 1018 steel.

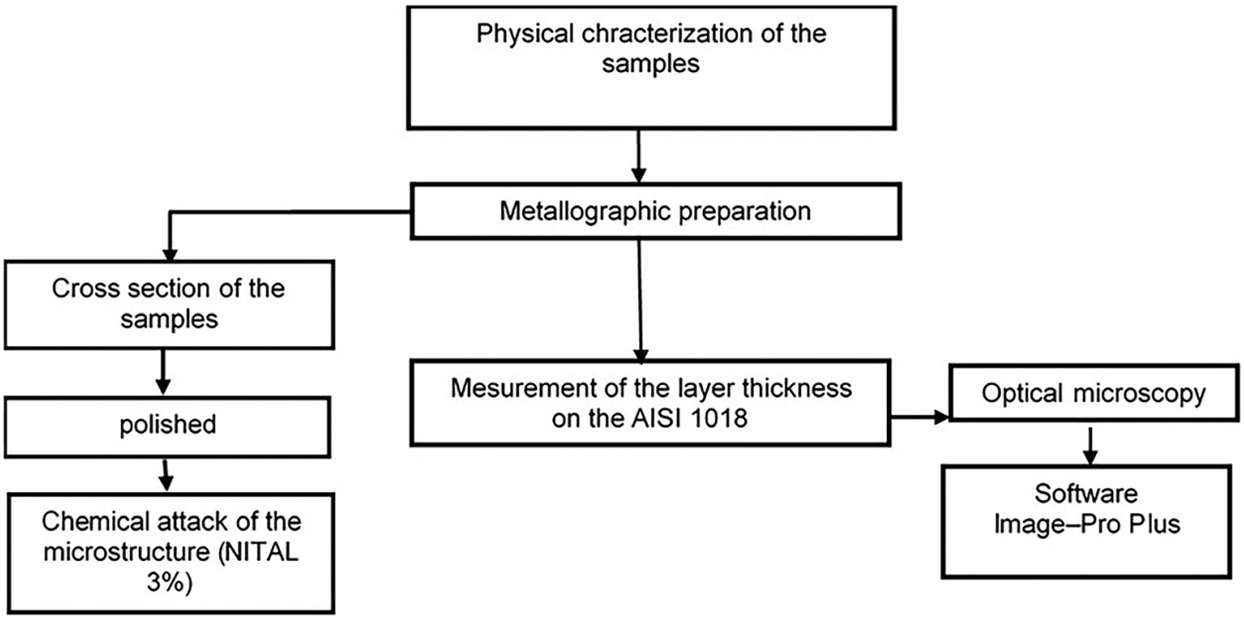

Figure 7. Flux diagram of the physical characterization of the AISI 1018 steel.

1.5.5. Layers thickness measurement

The measurement of the layer thickness was realized through the digitization of microscopy images by means of specialized software of image analysis.

Figure 8 shows the methodology used for the measurement of the layer thickness of the Fe_2B layers. At least 50 measurements are recommended for each picture in order to achieve a reliable value of the thickness.

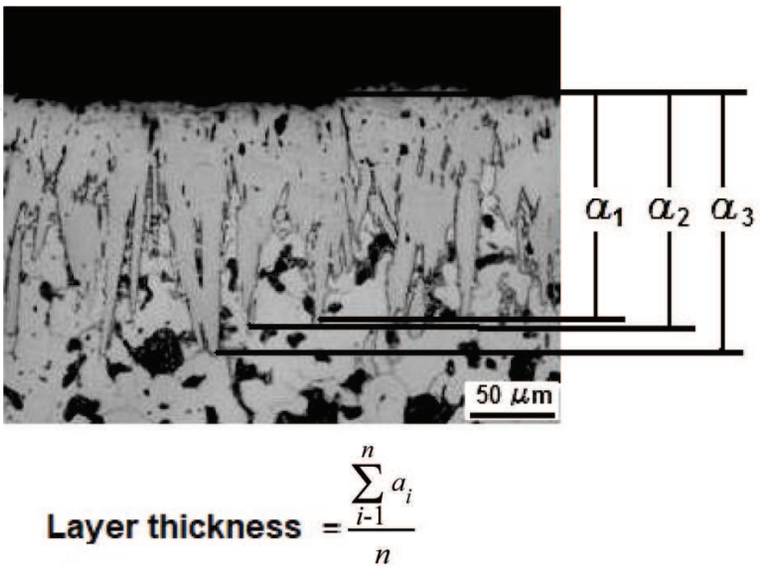

Figure 8. Methodology for the layer thickness measurement.

1.6. Results and discussion

1.6.1. Layer thickness

The layer thickness was obtained by the methodology described in **Figure 8**. Each numerical value of layer thickness was the result of the average of at least 50 measurements and the results are shown in **Table 3**.

Temperature. (K)	1.5 h	3 h	5 h
1173	32.51 ± 3.92	58.57 ± 6.27	73.96 ± 6.24
1223	45.37 ± 5.11	67.05 ± 10.28	86.02 ± 7.23
1273	48.55 ± 4.22	76.82 ± 6.67	97.84 ± 10.01

Table 3. Layers thickness of Fe_2B (μm) obtained for the different treatment conditions of time and temperature.

Figure 9 shows the evolution of the layer thickness as a function of the temperature and treatment time, according to Eq. (14).

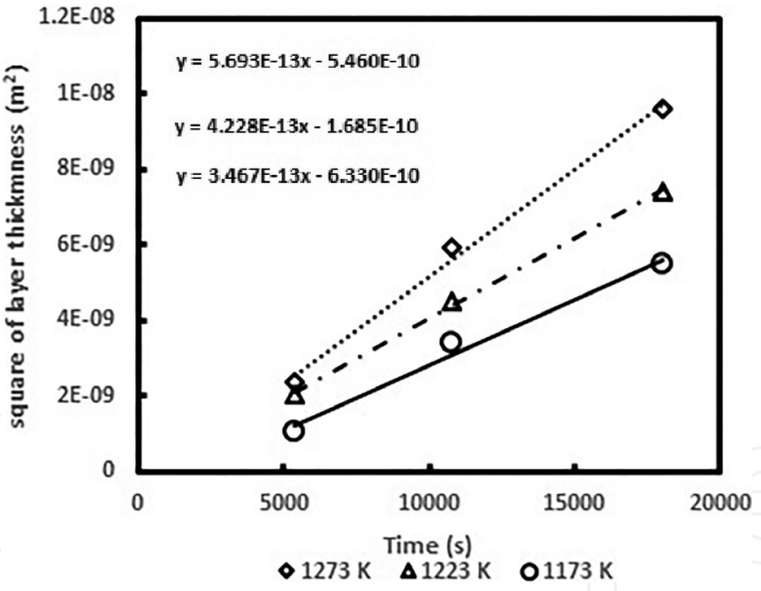

Figure 9. Evolution of the layer growth as a function of the different treatment conditions.

According to the results, the growth of the layers is described by a parabolic function (Eq. 14). The slopes of the lines obtained from **Figure 9** represent the constants of parabolic growth K, which indicates a controlled growth [1, 8, 14, 15].

Table 4 shows the values of the parabolic growth constant K, which were obtained from the slopes of the straight lines shown in **Figure 9**.

Temperature (K)	K (m^2 s^{-1})	1/T	Ln K	K_0	Q (KJ/mol)
1173	3.47E-13	8.53E-04	−2.87E + 01	1.8383E-10	61.3719122
1223	4.23E-13	8.18E-04	−2.85E + 01		
1273	5.69E-13	7.86E-04	−2.82E + 01		

Table 4. Constant of parabolic growth (K) and parameters for calculation of activation energy.

1.6.2. Estimation of the activation energy

Interstitial diffusion occurs when the atoms move from an interstitial position to another unoccupied neighbor but without permanently displacing any of the atoms in the crystalline network of the solvent. In general, less energy is required to displace an interstitial atom from the surrounding places. Consequently, the activation energy necessary for the process is smaller for interstitial diffusion than for vacancy or substitutional diffusion.

The activation energy necessary to make the process occur can be obtained by applying an Arrhenius-type expression (Eq. 16), as shown in **Figure 10**. As one can observe, from the plotting of the Eq. 16 (**Figure 10**), the slope of the straight line resulting of the graph can be used for the calculation of the activation energy as follows:

$$m = \frac{Q}{R} \tag{19}$$

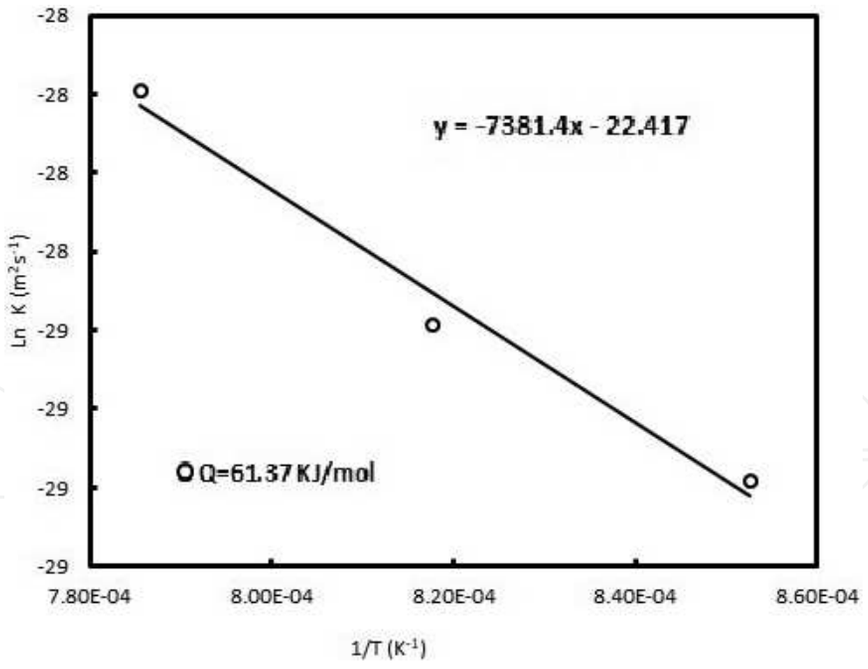

Figure 10. Behavior of the constant of parabolic growth as a function of the treatment temperature.

According to Eq. (19), activation energy can be estimated as:

$$Q = m*R$$

Then, by substituting the values of m and R:

$$Q = (7381.4)(8.3144)$$

The estimated activation energy value for the formation of the Fe_2B layer on the AISI 1018 steel surface was 61.37 KJ/mol. This value was compared with those obtained by different studies for different boriding steels (**Table 5**).

Material	Boriding method	Faces in the layer	Layer morphology	Activation energy, kJ/mol	Reference
AISI W1	B_4C powder	FeB, Fe_2B	Flat	171.2	[16]
AISI 5140	Salt bath	FeB, Fe_2B, CrB, Cr_2B	Saw-toothed	223	[1]
AISI 4340			Saw-toothed	234	
AISI D2			Flat	170	
AISI H13	B_4C paste	FeB, Fe_2B, CrB, Cr_2B	Flat	186.2	[17]
AISI 4140	Salt bath	FeB, Fe_2B, CrB	Saw-toothed	218.4	[12]
AISI 1018	B_4C paste	Fe_2B	Saw-toothed	161.82	[11]
AISI 1018	B_4C Powder	Fe_2B	Saw-toothed	61.37	Present work

Table 5. Values of the activation energy obtained for different steels exposed to boriding.

As can be seen in **Table 5**, the activation energy is also a function of the chemical composition of the substrate exposed to boriding, so that it increases as the alloying elements in the substrate increase.

The pre-exponential factor (K_0) can be also achieved from the **Figure 10** as shown in **Table 4**.

According to the results obtained from the **Figure 10**, Eq. (17) can be re-written as:

$$x = \sqrt{1.84E-10 \exp\left(-\frac{61371.9122}{8.3144T}\right)(t)} \tag{20}$$

Eq. (20) can be used to estimate the layer thickness as a function of the experimental conditions of time and temperature.

Table 6 compares the experimental values of the layer thickness and those estimated by Eq. (20) after determining the activation energy Q and the pre-exponential constant K_0 values for the treatment conditions.

Temperature. (K)	1.5 h		3 h		5 h	
	Experimental	By model	Experimental	By model	Experimental	By model
1173	32.51 ± 3.92	39.98	58.57 ± 6.27	56.55	73.96 ± 6.24	73.01
1223	45.37 ± 5.11	45.61	67.05 ± 10.28	64.5	86.02 ± 7.23	83.26
1273	48.55 ± 4.22	51.48	76.82 ± 6.67	72.8	97.84 ± 10.01	93.99

Table 6. Comparison between the experimental values of layer thickness (μm) and those obtained by applying the Eq. 20.

Table 6 shows a good agreement between the experimental values and those obtained from Eq. (20). These results indicate that it is possible to optimize the boriding process in industrial applications.

1.6.3. Contour diagram

Based on Eq. (20), it is possible to generate a contour diagram that represents the evolution of the layer thickness as a function of the experimental parameters, as shown in **Figure 11**.

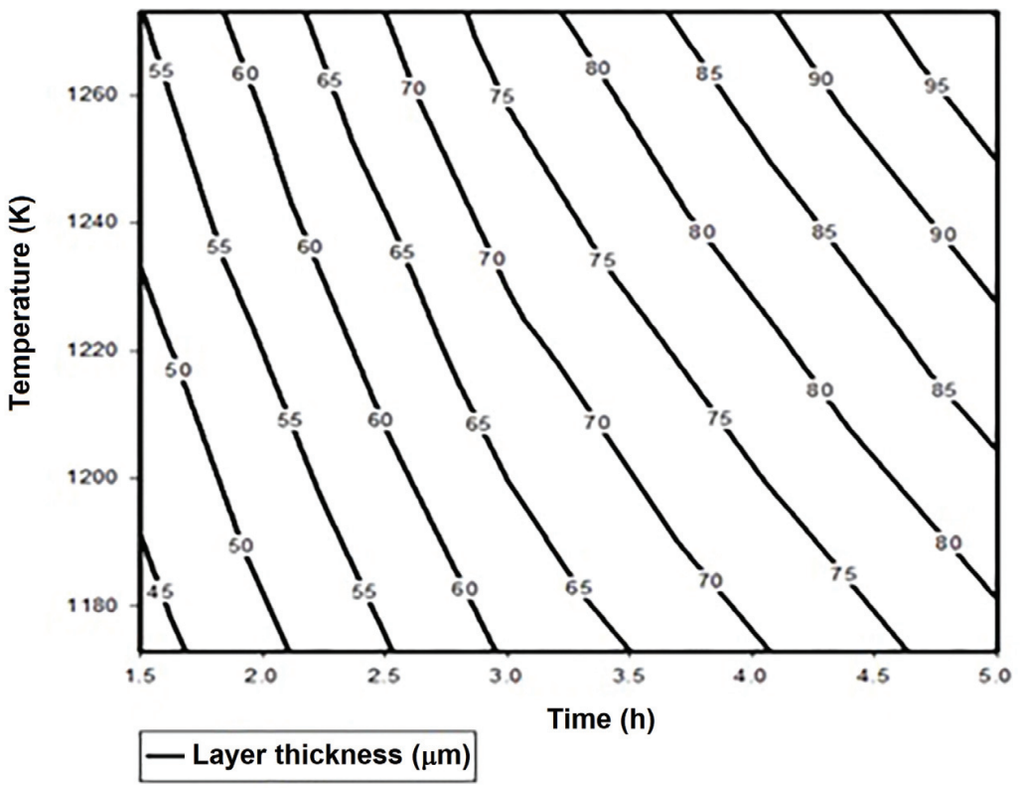

Figure 11. Contour diagram for the estimation of the layer thickness as a function of the experimental conditions.

Contour diagrams like these are especially useful in industrial applications, where representative process schemas are required to estimate quickly and reliably the desired layer thicknesses for a particular application.

1.7. Conclusions

According to the results, it is possible to observe that the layer thickness increases as the temperature and the treatment time increases, so the layer growth can be controlled.

The behavior of the parabolic growth constant as a function of the treatment temperature was established to determine the activation energy required for the formation of the boride layer on the surface of the AISI 1018 steel. Likewise, the boriding mixture used for the formation of the surface layer was enough to supply the required boron at different treatment conditions of time and temperature.

Finally, the growth of the Fe_2B layers on the surface of the AISI 1018 steel was represented by a contour diagram that establishes the time and temperature conditions of the boriding process, which helps to ensure the optimization of the process for superficially hardened low-carbon steels.

Author details

Enrique Hernández-Sánchez[1]* and Julio Cesar Velázquez[2]

*Address all correspondence to: enriquehs266@yahoo.com.mx

1 Instituto Politécnico Nacional-UPIBI, México City, México

2 Departamento de Ingeniería Química Industrial, ESIQIE, Instituto Politécnico Nacional, México City, México

References

[1] Sen S, Sen U, Bindal C. An approach of kinetic study of borided steels. Surface and Coatings Technology. 2005;**191**(2–3):274-285. DOI: http://doi.org/10.1016/j.surfcoat.2004.03.049

[2] Hernández Sánchez E. CARACTERIZACIÓN DE ACEROS BORURADOS AISI H13 [Thesis]. México: Instituto Politécnico Nacional. SEPI-ESIME; 2008. p. 145

[3] Von Matuschka AG. Boronizing. 1st ed. Germany: Carl Hanser Verlag; 1980. p. 97

[4] Campos Silva IE. Cinética de Difusión en el Proceso termoquímico de Borurización en aceros estructurales, de Baja Aleación, Herramientas e Inoxidables [thesis]. México: Universidad Autónoma Metropolitana; 1994. p. 165

[5] Campos I, Ramírez G, Figueroa U, Martínrz J, Morales O. Evaluation of boron mobilty on the faces FeB, Fe_2B and diffusion zone in AISI 1045, and M2 steels. Applied Surface Science. 2007;**253**(7):3469-3475. DOI: https://doi.org/10.1016/j.assusc.2006.07.046

[6] Palombarini G, Sambogna G, Carbucicchio M. Pole of Oxygen in iron boriding using boron carbide. Journal of Materials Science Letters. 1993:741-742. DOI: 10.1007/BF00626705

[7] Fisher C, Schaaber R. Proceeding of heat treatment. The Metals society. 1976;**76**:27-30

[8] Campos I, Oseguera J, Figueroa U, García JA, Bautista O, Kelemenis G. Kinetic study of boron diffusion in the pasts boriding process. Materials Science and Engineering. 2003; **352**(1–2):261-265. DOI: https://doi.org/10.1016/S0921-5093(02)00910-3

[9] Melendez E, Campos I, Rocha E, Barron MA. Structutal and Strength Characterization. Materials Science and Engineering: A. 1997;**234-236**:900-903. DOI: https://doi.org/10.1016/S0921-5093(97)00389-4

[10] Campos Silva I, Ortiz Domínguez M, Cimenoglu H, Escobar Galindo R, Keddam M, Elias Espinosa M, López Perrusquia N. Diffusion model for growth of Fe_2B layer pure iron. Surface Engineering. 2009;**27**(3):189-195. DOI: 10.1179/026708410X12550773057820

[11] Villa Velázquez Mendoza C. Estudio del Agrietamiento Tipo Palmqvist y Evaluación de Esfuerzos Residuales en Aceros Borurados AISI 1018 [thesis]. México: Instituto Politécnico Nacional-ESIME; 2009. p. 209

[12] Sen S, Sen U, Bindal C. The growth kinetic of borides formed on boronized AISI 4140 steel. Vacuum. 2005;**77**(2):195-202. https://doi.org/10.1016/j.vacuum.2004.09.005

[13] Vipin J and Sundararajan G. Influence of the pack thickness. Surface and Coatings Technology. 2002;**149**(1):21-26. https://doi.org/10.1016/S0257-8972(01)01385-8

[14] Campos I, Ramírez G, Figueroa U, Villa VC. Paste boriding process evaluation of boron mobility on borided steels. Surface Engineerin. 2007;**23**(3):216-222. http://dx.doi.org/10.1179/174329407X174416

[15] Campos-Silva I, Ortíz-Domínguez M, López Perrusquia N, Escobar-Galindo R, Gómez-Vargas OA, Hernández-Sánchez E. Determination of boron diffusion coefficients in borided tool steels. Defect and Diffusion Forum. 2009;**283-286**:681-686. DOI: 10.4028/www.scientific.net/DDF.283-286.681

[16] Genel K, Ozbek I, Bindal C. Kinetics of boriding of AISI W1 steel. Materials Science and Engineering: A. 2003;**347**(1–2):311-314. https://doi.org/10.1016/S0921-5093(02)00607-X

[17] Genel K. Boriding kinetics of H13 steel. Vacuum. 2006;**80**(5):451-457. DOI: 10.1016/j.vacuum.2005.07.013

IntechOpen